



INTERNATIONAL JOURNAL OF
RESEARCH IN COMPUTER
APPLICATIONS AND ROBOTICS
ISSN 2320-7345

MODELING OF BIOLOGICAL CONTROL SYSTEMS ESTABLISHED BETWEEN HUMAN BRAIN NEURONS

Sibiri TRAORE (Ph. D.)

Department of Mechanical Engineering
Institut Pédagogique National de l'Enseignement Technique
et Professionnel (IPNETP) - Côte d'Ivoire

Abstract

In terms of structure, the complexity of the interconnections between neurons in the human brain is well established. A study of these interconnections shows that some are particularly similar to feedback loop control systems used in engineering to control certain production devices. These biological control systems are encountered between neurons belonging to the same macrostructure, or between different macrostructures of the human brain. They are involved in the control or regulation of several biological phenomena such as: hormonal secretions, temperature, body posture, coordination of movements, emotions, reasoning, decision-making, etc. The artificial intelligence research work presented in this paper concerns the mathematical modeling of these natural control systems with feedback loops. The objective is to contribute to the development of intelligent systems used to control the movement and behavior of robots, giving them the capacity and autonomy to react and adapt to changes in their environment, in a manner analogous to physiological homeostasis. After describing briefly the physiology and the structural organization of biological neurons, architecture and algorithm are designed to illustrate the behavior of some simple feedback control systems found in human brain. Then, simulations are carried out to validate the artificial model. The results show that the use of Artificial Intelligence (AI) improves the accuracy, efficiency and flexibility of feedback control systems in industrial process automation. In terms of perspectives, other models will be designed and combined with existing models, including this one, to produce reasoning and decision-making; which would allow robots to analyze situations and interact intelligently with their environment. This work can also serve as a reference for researchers and professionals interested in the development and applications of AI-inspired feedback control systems.

Keywords: neuron, control system, synapse, action potential, frequency, amplitude.

Introduction

As part of our research into artificial intelligence, we have been working for several years on the ambitious project of designing mathematical models of the main components and

functions of the human brain. The goal is to provide production systems, particularly robots, with intelligence and autonomy when performing certain tasks. In other words, we want the machines in question to be intelligent, like humans, through their ability to analyze situations, reason, and make decisions before acting when handling industrial products.

To achieve this goal, in a first article [18], we developed an algorithm that is a model of the electrophysiology of neurons in the human brain. This algorithm has proven itself for learning relatively simple data, as is done with other types of neural networks ([2], [5], [8], [9], [11], [12], [13], [15], [16], [17], and [19]). According to the neurobiology literature ([3], [4], [6], [7] and [14]), learning is not the only function of the human brain essential to the accomplishment of intelligent behaviors. Among many others, the brain is also involved in the regulation of various physiological phenomena that allow the control of homeostasis (or general balance) of the human body and in the development of human intelligence.

The processes involved in the realization of these physiological phenomena are complex and involve different brain areas with specific functions. It is therefore not an isolated act of a single part of the brain, but a collaborative effort of several macrostructures such as the cortical areas, the hippocampus, the hypothalamus, the thalamus, the basal ganglia, the cerebellum, the spinal system, etc. Thus on the architectural level, we note that the neurons are interconnected in a very complex way, forming a dense network that is difficult to describe as a whole. But specifically, particular types of connections or neuronal circuits, similar to feedback loops, are observable between certain neurons of the same macrostructure, or even between distinct macrostructures.

Such circuits are similar to control systems used for controlling various industrial processes and play a very important role in the physiology of the human body. They are used to regulate body temperature, heart rate, breathing rate, hormonal secretions, eating behavior, emotions, desires, situation analysis, reasoning, decision-making, coordination of movements, posture, muscular effort, etc.

In artificial intelligence, models of these biological servomechanisms must be developed, taking into account the specific role they play, and interconnected to form circuits capable of performing situation analysis, reasoning, and decision-making at the level of robot control systems. Our study, based on the algorithm developed in [18], therefore focuses on modeling simple cases of these feedback loop control systems observed in the human brain, and is structured as follows:

- a) Section 2 provides a brief schematic and functional description of these control systems, both at the neuronal and macrostructural levels;
- b) Section 3 uses the algorithm developed in [18] to illustrate the operation of a simplified model of the control system. At this level, the algorithm is once again validated, not in terms of learning, but for process control;
- c) Finally, curves resulting from simulations are presented to illustrate the model's behavior.

1. Methodology

Three stages are necessary to complete this work:

- 1) First, a brief overview is given of the nature of information and the mode of communication between neurons, in terms of nerve impulses and the electro-biochemical

process involved in its transmission from a presynaptic neuron to a postsynaptic neuron. It is also necessary to highlight the specific neural or macrostructural interconnections similar to feedback loop control systems.

2) Drawing inspiration from the first part of the study, in the second part, a simple servomechanism architecture with a feedback loop similar to its biological counterpart is developed. Next, an algorithm is formulated to illustrate the flow and processing of information through this servomechanism.

3) Finally, in terms of results, several simulations are performed to validate the model.

2. Results

2-1. Control systems observed in the human brain

Before describing the control systems in the nervous system, it is important to briefly review how nerve impulses circulate through neurons. This review is intended to convey the scope of the project and facilitate understanding of the algorithm used.

2-1-1. Nerve impulse circulation

As described in [14], when a neuron is at rest, a potential difference, called the resting potential, negatively polarizes the interior of the nerve cell relative to the extracellular medium. When a stimulus excites the resting neuron, the resting potential reverses abruptly and locally, giving rise to a nerve impulse called an action potential, which propagates along the entire length of the neuron, at a given amplitude and frequency.

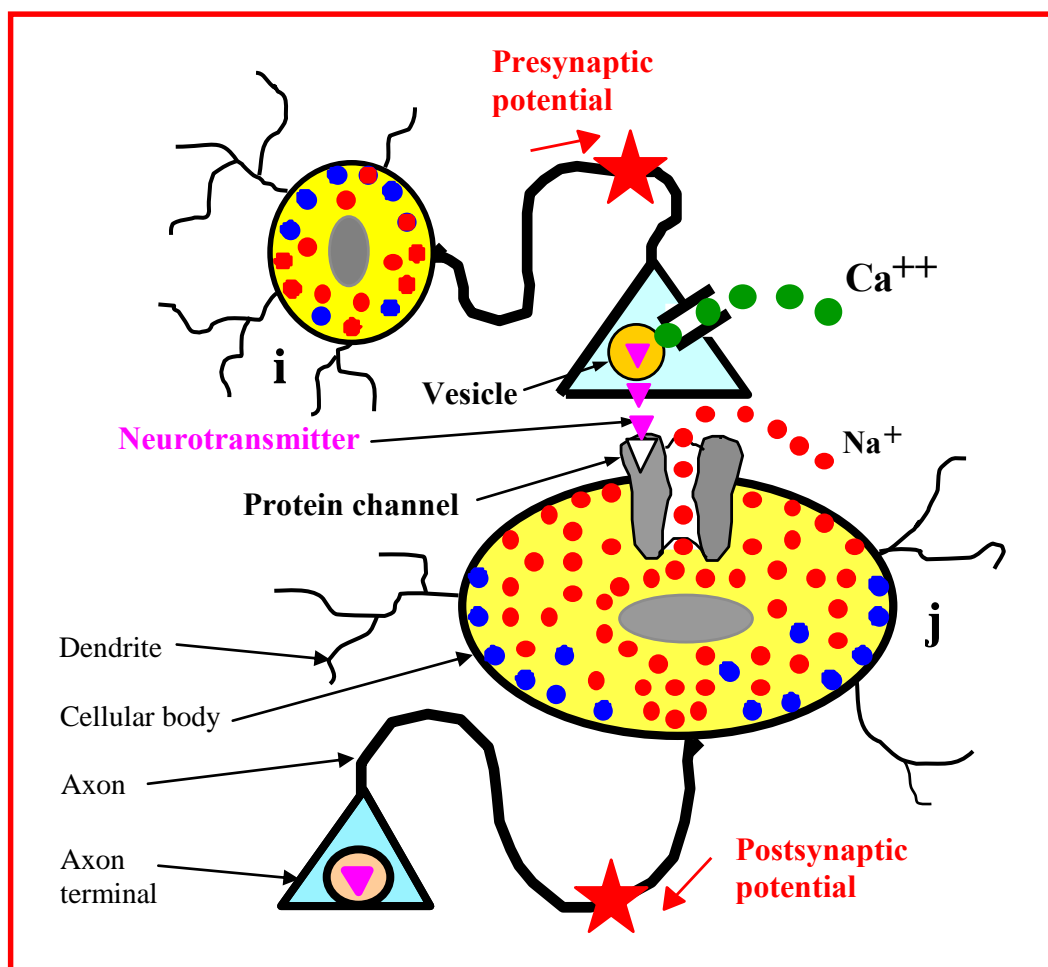
When the nerve impulse from presynaptic neuron i arrives at an axon terminal, it is transmitted to postsynaptic neuron j via synaptic contact. This inter-neuronal transmission of the nerve impulse is not direct. The process behind the induction of postsynaptic nerve impulses, following the arrival of the presynaptic nerve impulse at the presynaptic axon terminals, is biochemical and complex. This process is divided into several stages according to the following chronology (Figure 1):

- a) In the axon terminal, the synthesis of mediator (or neurotransmitter) molecules is carried out by the biochemical substances of the presynaptic neuron even before their release into the synaptic space;
- b) After synthesis, the mediator molecules are stored in the axon terminals within small synaptic vesicles, which are themselves connected to each other by action filaments;
- c) The arrival of a nerve impulse causes the calcium channel proteins located on the membrane of the axon terminal to open to allow the passage of calcium ions (Ca^{++}) existing in the extracellular medium;
- d) Ca^{++} ions react with the medium to break the bond between the vesicles by dissolving the action filaments, and cause them to move towards the membrane of the axon terminal bordering the synaptic space. At this level, the vesicles fuse with the channel proteins of the membrane, followed by the release of a large number of neurotransmitter molecules into the synaptic space;

- e) The released molecules diffuse rapidly into the fluid occupying the synaptic space, then bind to neuroreceptors in the membrane to cause the opening of the protein channels of the postsynaptic neuron j;
- f) The opening of the protein channels of the postsynaptic neuron j promotes ion exchange between the intracellular and extracellular environments. This ion exchange causes a sudden reversal of the resting potential, which corresponds to the induction of the postsynaptic action potential (or nerve impulse).

This process can occur several times per second, with constant amplitude along the entire length of the neuron. The number of times it occurs is called the action potential frequency.

Figure 1: Illustration of synaptic biochemical events.



2-1-2. Feedback control systems between neurons

Figure 2 below represents a simplified model of a feedback control system observed between certain neurons in the same macrostructure. It is composed of four neurons i, j, k, and d and operates as follows:

- a) A given stimulus innervates presynaptic neuron i to achieve a goal (e.g., lifting an object with the arm);

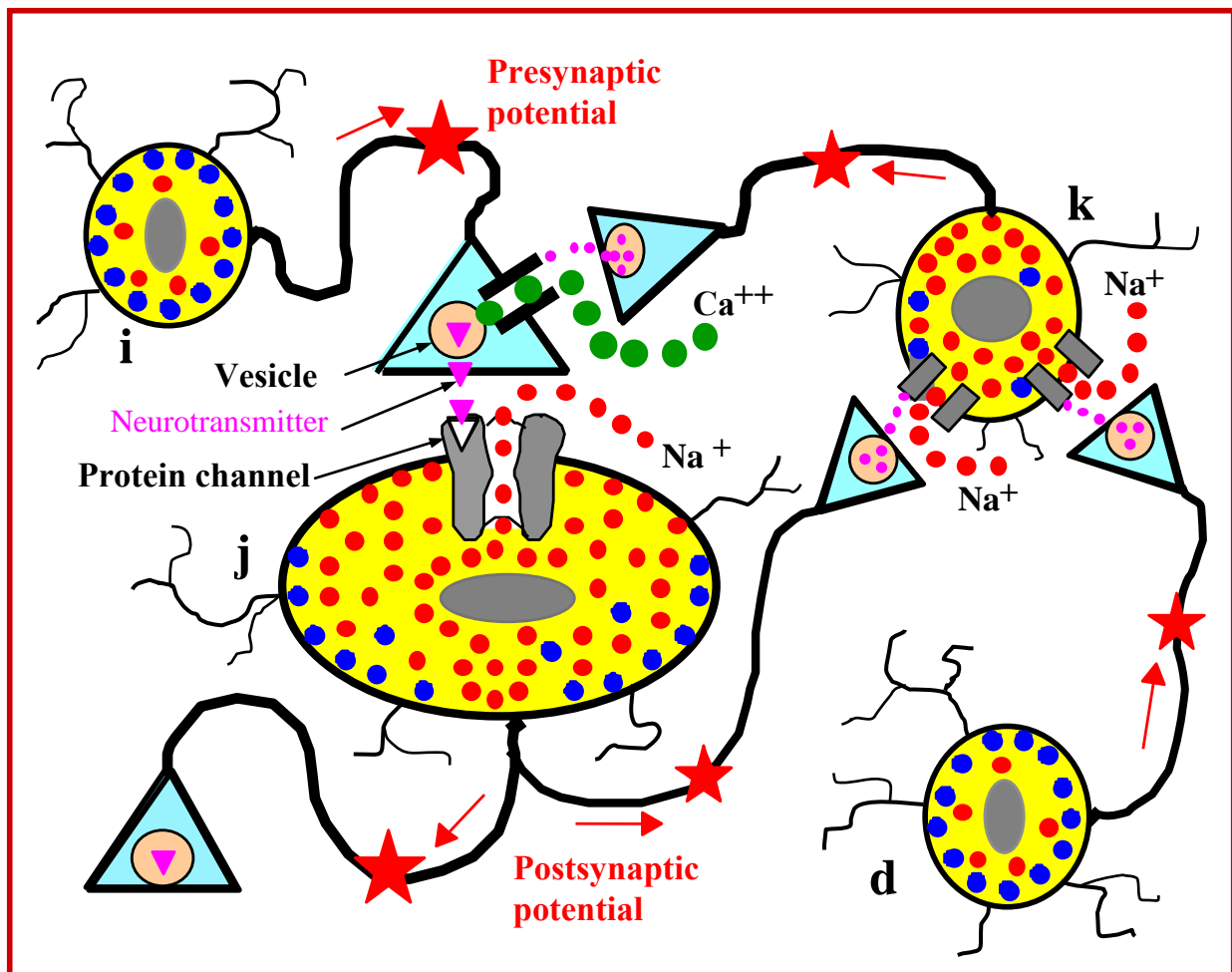
- b) Following stimulation of this presynaptic neuron i, a nerve impulse is induced and propagates along the entire length of the neuron to the axon terminal;
- c) At the axon terminal, neurotransmitters are released into the synaptic space according to a biochemical mechanism already explained above;
- d) These neurotransmitters then bind to the protein channels of postsynaptic neuron j to cause these protein channels to open;
- e) Open protein channels allow Na^+ ions to pass into the cell body of the postsynaptic neuron j. This induces a postsynaptic action potential, which also propagates to the axon terminals. One of the axon branches transmits this impulse to the effector (e.g., the arm), while another branch transmits the impulse to neuron k, which compares the action potential of neuron j with the desired action potential provided by neuron d (the action potential of neuron d is the one required for the effector to act in accordance with the programmed movement).
- f) The integration of the effects of the two action potentials of neurons j and d at neuron k induces an action potential that would correspond, hypothetically, to the potential difference between the desired action potential at the output of neuron d and the action potential obtained at the output of neuron j. In other words, the action potential at the output of neuron k would, hypothetically, be equivalent to a difference in action potential.
- g) At the axon terminal of neuron k, the effect of this potential difference is to trigger the release of specific neurotransmitters into the synaptic space formed by the axon terminals of neurons i and k.
- h) These neurotransmitters bind to calcium channel proteins. Depending on whether their effect is to increase or decrease the action potential of neuron j, they promote the opening or closing of calcium channel proteins to allow or prevent the passage of Ca^{++} calcium ions. In other words, the effect of the action potential of neuron k is to contribute to the process of releasing neurotransmitters into the synaptic space between neurons i and j, combining this effect with that of the action potential of neuron i, in the sense of regulating the nerve impulse of neuron j.
- i) If necessary, the process described in steps 1 to 8 is repeated iteratively until the output potential of neuron j and the output potential of neuron d are identical in value. In other words, this results in the action potential of neuron k becoming zero. This zero value corresponds to stability in the functioning of the biological servomechanism as a whole. Such stability is absolutely impossible, given the phenomena of fatigue and irregularity in ion exchanges at all synaptic levels. Stability would therefore be relative within a tolerance interval where oscillations around the level of absolute stability are observed and result from the iterative process of regulating biochemical activity and, consequently, the behavior of the effector.

Note

Figure 2 below illustrates the complexity with which neurons are interconnected and communicate with each other. Some connections are similar to feedback loop

servomechanisms. This highlights the difficulties involved in modeling electro-biochemical events at the synaptic level. These difficulties stem from the mathematical translation of the presynaptic action potential into presynaptic biochemical events related to neurotransmitter release, the mode of diffusion of neurotransmitters in the synaptic space, the mode of their selective binding to postsynaptic neuroreceptors, the direct or indirect process of opening or closing postsynaptic channel proteins, and the induction of the postsynaptic potential. Furthermore, we do not know how many neurotransmitters are released into the synaptic space, how many channel proteins are open or closed for the passage of ions at the postsynaptic neuron, and how many ions are exchanged between the ambient environment and the interior of the neuron. These difficulties can be overcome in modeling by making simplifying assumptions.

Figure 2: Simplified model of a feedback control system between neurons of the same macrostructure. This model illustrates how the electrobiochemical activity of neuron j is regulated by neurons i and k. Neuron d provides the desired output potential for j.



2-1-3. Feedback control systems between macrostructures

Between the different macrostructures that make up the nervous system, several types of control systems are observed, ranging from the simplest to the most complex connections. For example, with regard to motor actions, there are two types of control systems: open-loop

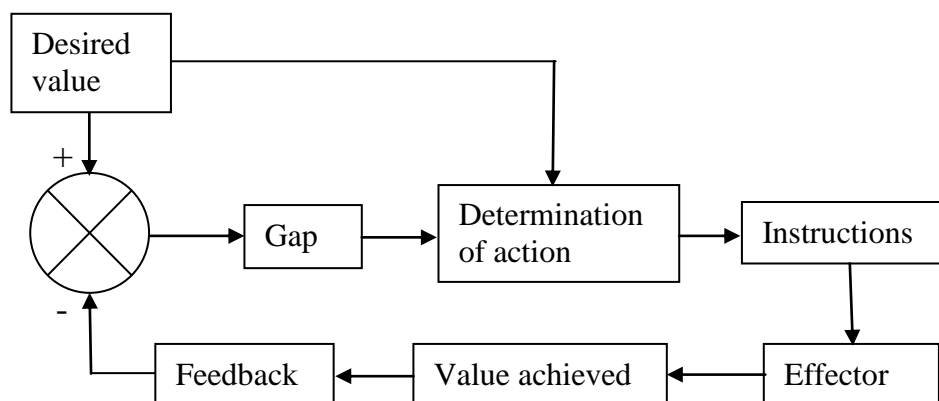
control systems and closed-loop control systems. It is the latter type of loop that concerns us at the moment.

The closed-loop control system relies on the use of feedback (Figure 3). The movement is corrected as it progresses [6]. The temperature control system in a house using a thermostat is a perfect example of this type of control: the desired temperature is first set on the thermostat, which simultaneously measures the ambient temperature and the difference between the two temperatures; when the desired temperature is lower than the ambient temperature, the difference (or error) triggers an instruction to the heating (or air conditioning) system, which starts up and operates as long as this difference remains negative. When the difference becomes zero and tends to be positive, the system gives the command to stop.

Such a system constitutes a closed-loop or error-reduction servomechanism. It relies on the detection of a difference (or error) and on feedback that instructs the control system on the similarity or difference between intention and action. Thus, when performing a movement, for example, proprioceptive, visual, or somatosensory sensations provide feedback on its progress, based on which it is possible to correct or modify the movement.

When picking up an object from a table, for example, the trajectory of the arm and hand is controlled at every moment by feedback from visual and proprioceptive afferents. This point-by-point processing of information requires that it be fast enough for the system to take into account reafferents and detect errors, develop and implement corrections. When a movement becomes too fast, this progressive or chain mode of control is no longer possible. Only continuous control of slow or ramp movements can be performed in a closed loop.

Figure 3: Closed-loop motion control type, [14].



2-1-4. Central movement control system

As described in the steps below, the central movement control system model (Figure 4) distinguishes between movement planning and programming functions and program execution and control functions:

Step 1: Idea of movement

The idea of movement arises from a process that stems from the feeling of an emotional need, a need for survival, external stimulation from our environment, or the desire to solve a problem. It essentially involves the hypothalamus in relation to other substructures.

Step 2: Decision to perform the movement

The decision to perform the movement involves components such as the thalamus and limbic system, which are the centers of motivation. At this level, our degree of motivation determines whether or not we decide to perform the movement.

Step 3: Movement planning

As soon as the decision to perform the movement is made, the frontal and parietal associative cortical areas are the first to be informed. They contribute to movement planning: image of the goal to be achieved, anticipation of re-references and succession of different phases. The frontal cortical areas regulate the subject's motivational context and interest in the goal of the movement. The parietal cortical areas act more in the spatial context by developing a strategy that varies according to the position of the target of the movement in relation to the body.

Step 4: Movement programming

Recordings have shown that neurons linked to attention, task, or strategy, through loops that engage the parietal areas, motor cortex, basal ganglia, and cerebellar hemispheres (neocerebellum), identify the components of motor programming and postural support movements that facilitate it. The cerebellum and spinal cord are also involved in developing the movement program for establishing or anticipating the basic muscle activity that facilitates movement execution. They participate in movement regulation. Information relating to the movement program is then transmitted to the frontal motor cortex.

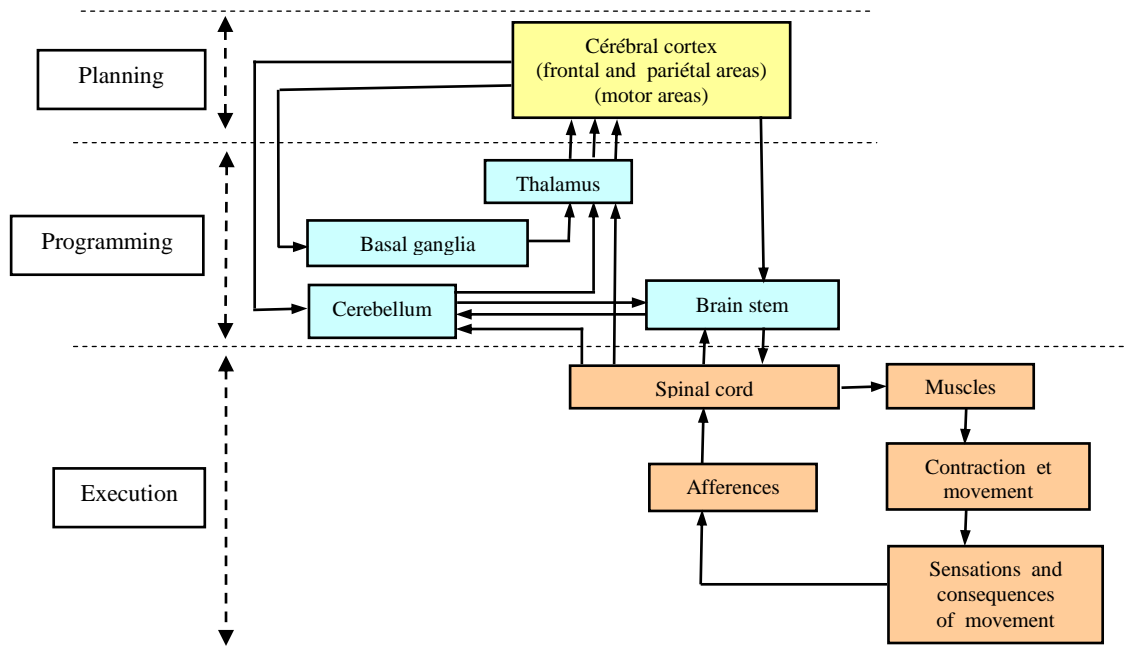
Step 5: Execution of the movement

As soon as the movement program data reaches the motor cortex, it is transformed into motor nerve impulses and sent to the relevant motor nuclei in the spinal cord. Then, the movement begins: muscle contractions or extensions, force and speed of the moving element, somatosensory sensation, afference (feedback on the movement for correction or otherwise).

Step 6: Movement correction

If it is a known ballistic movement, it takes place without peripheral assistance, as it is preprogrammed very precisely. In the case of a slow ramp movement, medullary or cortical assistance loops contribute to its regulation. Short medullary loops obey the principle of coactivation, and neuromuscular spindles contribute to the local terminal adjustment of the central program with a minimal margin of error.

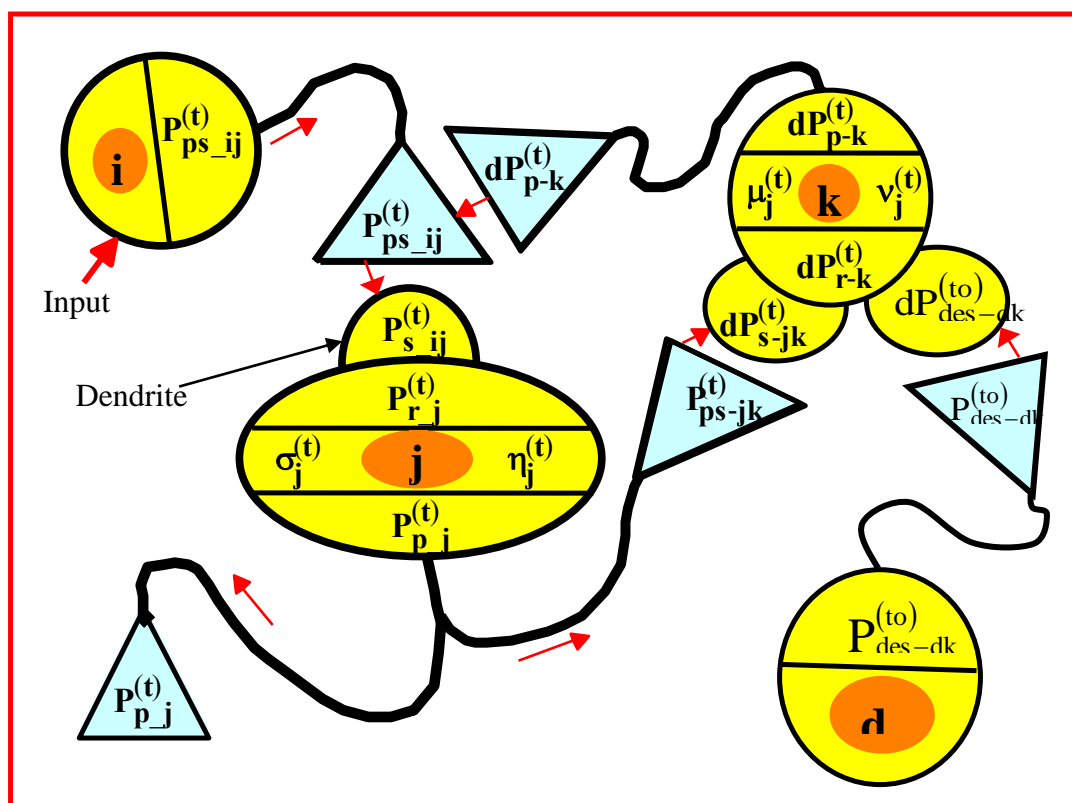
Figure 4: Simplified model of the motion control system. Several closed-loop subsystems combining the components involved in motion planning, programming, and execution can be identified.



2-2. Presentation of the artificial feedback control system algorithm

Figure 5 below corresponds to a parameterized model of the biological feedback control system observed between neurons of the same macrostructure shown in Figure 2.

Figure 5: Parameterized model of the feedback control system observed between biological neurons.



Several elements must be considered when modeling the biological feedback control system, [18]:

a) Architecturally speaking, the aim is to establish a similarity between the biological control system shown in Figure 2 above and its artificial model. This is why Figure 5 below shows a control system model that is directly inspired by the one in Figure 2. These two similar figures show the connection between neurons i, j, k, and d in the form of a servomechanism with a feedback loop. This type of architecture is then used to formulate the algorithm.

b) At the level of the natural neuron, nerve impulses travel in a unidirectional manner from the dendrites to the axon terminals. To optimize the differences (or errors) between the output information of neuron j and the desired output, rather than developing a model such as the Multilayer Perceptron ([2], [9], [15]), where impulses flow in both directions, the model proposed here takes into account the single directionality of impulse flow at the biological neuron level. This unidirectionality justifies the closed-loop configuration of the control system through the use of neurons k and d. The algorithm is therefore divided into two parts: the first part concerns neurons i and j for data processing, and the second part concerns neurons k and d for optimizing deviations.

c) With regard to the mathematical translation of the electro-biochemical events that characterize the induction of nerve impulses, it is known from the previous sections that the impulse traveling through a presynaptic neuron propagates at a given frequency and amplitude. This impulse causes the release of neurotransmitters, which in turn cause, through electro-biochemical events, the subsequent induction of nerve impulses in the postsynaptic neuron. Since these electro-biochemical events are not quantitatively known, it is difficult to establish a direct and explicit relationship between the presynaptic impulse and the postsynaptic impulse. To achieve this, based on hypotheses, the presynaptic nerve impulse, defined in terms of amplitude and frequency, is transformed into a postsynaptic nerve impulse according to parameters or functional relationships.

2-2-1. Definition of neurons parameters

a) Parameters relating to the nerve impulse (or electrical potential) of neuron i:

$A_{ps-ij}^{(t)}$ amplitude of the impulse from presynaptic neuron i to postsynaptic neuron j;

$f_{ps-ij}^{(t)}$ frequency of the influx from presynaptic neuron i to postsynaptic neuron j.

b) Parameters relating to the nerve impulse of neuron j:

$A_{s-ij}^{(t)}$ amplitude of the synaptic impulse generated by i at j;

$f_{s-ij}^{(t)}$ frequency of synaptic impulses generated by i at j;

$A_{r-j}^{(t)}$ amplitude of the resulting impulse generated by i at j ($i \geq 1$);

$f_{r-j}^{(t)}$ frequency of the resulting influx generated by i at j;

$A_{p-j}^{(t)}$ amplitude of the impulse specific to the output of neuron j;

$f_{p-j}^{(t)}$ frequency of the influx specific to the output of neuron j;

$A_{s-ij}^{(0)}$ resting amplitude (initial value) of neuron j;

- $\sigma_j^{(t)}$ sensitivity of neuron j to stimuli from other neurons i;
 $\eta_j^{(t)}$ amplification factor of the synaptic impulse of neuron j.

c) Parameters relating to the nerve impulse of neuron k:

- $dP_{s-jk}^{(t)}$ synaptic electrical potential difference generated by j at k;
 $dP_{des-dk}^{(to)}$ synaptic electrical potential difference generated by d at the level of k;
 $dP_{r-k}^{(t)}$ difference in electrical potential resulting at k;
 $dp_{p-k}^{(t)}$ electrical potential difference specific to the output of neuron k;
 $dA_{p-k}^{(t)}$ amplitude of the electrical potential difference specific to the output of k;
 $f_{p-k}^{(t)}$ frequency of the specific electrical potential difference at the output of k;
 $\mu_k^{(t)}$ sensitivity of neuron k to frequency variations;
 $v_k^{(t)}$ sensitivity of neuron k to amplitude variations.

d) Parameters relating to the nerve impulse of neuron d :

- $P_{des-dk}^{(to)}$ desired electrical potential at the output of neuron d;
 $dP_{des-dk}^{(to)}$ desired synaptic potential difference generated by d at the k level.

After defining the various parameters, the algorithm that characterizes the operation of the artificial feedback control system can be formulated in two parts as follows:

2-2-2. First part of the algorithm relating to neurons i and j

- 1) Fixed values are assigned to the sensitivity $\sigma_j^{(t)}$ and amplification factor $\eta_j^{(t)}$ of the postsynaptic neuron j. These values are chosen between 0 and 1, and modulate the nerve impulse through the postsynaptic neuron j.
- 2) A fixed initialization value is also assigned to the resting amplitude $A_{s-ij}^{(0)}$, (value between 0 and 1).
- 3) The input information of neuron j is defined in terms of frequency $f_{ps-ij}^{(t)}$ and amplitude $A_{ps-ij}^{(t)}$. The frequency $f_{ps-ij}^{(t)}$ at the output of neuron i is the data to be processed by neuron j, and the corresponding amplitude $A_{ps-ij}^{(t)}$ plays the same role as the weights w_{ij} in the Multilayer Perceptron algorithm [9]. The values of $A_{ps-ij}^{(t)}$ increase (or decrease) through the action of neuron k, so that the output information $f_{p-j}^{(t)}$ of neuron j converges towards the desired output value $f_{des-dk}^{(to)}$ of neuron d. At each iteration at time t, neuron k simultaneously receives the output potential of neuron j and that of neuron d, and processes them to provide a potential difference at its output. Since the

frequency at its output is assumed to be the same as that of neuron i , the amplitude of this potential difference modifies the input amplitude $A_{ps-ij}^{(t)}$ of neuron i at time $t + 1$.

Initial values are assigned to the input amplitudes $A_{ps-ij}^{(t)}$ before the first iteration.

- 4) We define the output information $f_{des-dk}^{(to)}$ of neuron d (the information that the output information of neuron j must reach).

- 5) At the synaptic contact, the presynaptic potential $P_{ps-ij}^{(t)}$ is expressed.

$$P_{ps-ij}^{(t)} = A_{ps-ij}^{(t)} f_{ps-ij}^{(t)} \quad (1)$$

- 6) Next, the induced synaptic potential $p_{s-ij}^{(t)}$ at neuron j is expressed.

$$P_{s-ij}^{(t)} = \sigma_j^{(t)} A_{ps-ij}^{(t)} f_{ps-ij}^{(t)} = \sigma_j^{(t)} P_{ps-ij}^{(t)} \quad (2)$$

- 7) The resulting action potential $P_{r-j}^{(t)}$ of neuron j is determined.

$$P_{r-j}^{(t)} = \sum_{i=1}^n P_{s-ij}^{(t)} = \sigma_j^{(t)} \sum_{i=1}^n A_{ps-ij}^{(t)} f_{ps-ij}^{(t)} \quad (3)$$

(where n is the number of synaptic contacts of neuron j . Here in Figure 5, $n = 1$).

- 8) The resulting amplitude $A_{r-j}^{(t)}$ of neuron j (which is also its output potential $P_{p-j}^{(t)}$) is determined.

$$A_{r-j}^{(t)} = A_{s-j}^{(0)} + \sum_{i=1}^n A_{s-ij}^{(t)} = A_{s-j}^{(0)} + \eta_j^{(t)} \sum_{i=1}^n A_{ps-ij}^{(t)} = A_{p-j}^{(t)} \quad (4)$$

- 9) The corresponding resulting frequency $f_{r-j}^{(t)}$ of neuron j is determined.

$$f_{r-j}^{(t)} = f_{r-j}^{(t)} / A_{r-j}^{(0)} = (\sigma_j^{(t)} \sum_{i=1}^n A_{ps-ij}^{(t)} f_{ps-ij}^{(t)}) / (A_{s-j}^{(0)} + \eta_j^{(t)} \sum_{i=1}^n A_{ps-ij}^{(t)}) \quad (5)$$

- 10) The output frequency $f_{p-j}^{(t)}$ provided by neuron j is expressed.

$$f_{p-j}^{(t)} = -1 + (2 / [1 + \exp(-f_{p-j}^{(t)} - \theta_j^{(t)})]) \quad (6)$$

(where $\theta_j^{(t)}$ is a constant between 0 and 1 to position the curve horizontally).

- 11) The output potential $P_{p-j}^{(t)}$ of neuron j is then determined.

$$P_{p-j}^{(t)} = A_{p-j}^{(t)} f_{p-j}^{(t)} \quad (7)$$

- 12) The difference between the desired output value of neuron d and that of neuron j is calculated.

$$\epsilon_j^{(t)} = f_{des-dk}^{(t)} - f_{p-j}^{(t)} \quad (8)$$

These initial equations characterize the induction of nerve impulses (action potential) at neuron j .

2-2-3. Second part of the algorithm relating to neurons k and d

As the first part of the algorithm is formulated, the output frequency $f_{p-j}^{(t)}$ of neuron j does not converge to the desired output frequency $f_{des-dk}^{(to)}$ at neuron j . In other words, we do not obtain a nullity of $\varepsilon_j^{(t)}$.

To obtain the nullity of $\varepsilon_j^{(t)}$, a complementary algorithm is developed for neurons k and d .

We assume that the non-convergence of $f_{p-j}^{(t)}$ towards $f_{des-dk}^{(to)}$ can be considered as a state of instability of the neural control system. Based on Lyapunov stability theory, this second part of the algorithm assigns neuron k the role of corrector (or regulator) of the amplitudes at the output of neuron i , and consequently at the input of neuron j .

Indeed, according to Lyapunov's stability theory [10], regardless of the number of iterations, the output information $f_{p-j}^{(t)}$ of neuron j must converge toward $f_{des-dk}^{(to)}$ of neuron d and remain stable (or relatively constant) within a tolerance interval defined in relation to $f_{des-dk}^{(to)}$ (see Figure 6 below). Even when disturbed by an external stimulus, the control system must therefore regain its stability (quickly).

If Φ is a function defined in terms of amplitude, the stability condition according to Lyapunov can be expressed as follows.

If, in general, neuron k has m outputs ($m = 1$ in Figure 5), each of which is associated with an output of neuron i , in order to modify the amplitude $A_{ps-ij}^{(t)}$ corresponding to $A_{p-k}^{(t)}$ of neuron k , this modification will be made as a function of time t (or the number of iterations in our case). In differential form, we can write the following general relationship:

$$\frac{dA_{p-k}^{(t)}}{dt} = \Phi_{p-k}^{(t)}(A_{p-1}^{(t)}, A_{p-2}^{(t)}, \dots, A_{p-k}^{(t)}, \dots, A_{p-m}^{(t)}, t) \quad (9)$$

A solution $\varphi_{p-k}^{(t)}$ of this equation satisfying the initial conditions $\varphi_{p-k}^{(t)} = \varphi_{p-k}^{(to)}$ is said to be stable in the Lyapunov sense for $t \rightarrow +\infty$ si, $\forall \lambda > 0, \exists \delta(\lambda) > 0 / \forall \varphi_{p-k}^{(t)}$ a solution of (9) whose initial values satisfy the conditions:

$$\forall t \geq t_0, \text{ si } |A_{p-k}^{(to)} - \varphi_{p-k}^{(to)}| < \delta(\lambda) \quad (10)$$

(where $\delta(\lambda)$ is an arbitrary value).

We have the inequality:

$$|A_{p-k}^{(t)} - \varphi_{p-k}^{(t)}| < \lambda \quad (11)$$

The solution $\varphi_{p-k}^{(t)}$ is said to be unstable if, for $\delta(\lambda) > 0$ however small it may be, inequality (11) is not verified for at least one solution $A_{p-k}^{(t)}$. If, under condition (10), and in addition to inequality (11), the following condition is verified:

$$\lim_{t \rightarrow +\infty} |A_{p-k}^{(t)} - \varphi_{p-k}^{(t)}| = 0 \quad (12)$$

The solution $\varphi_{p-k}^{(t)}$ is said to be asymptotically stable. It is this asymptotic stability that we seek for the output information $A_{p-k}^{(t)}$ of neuron k. If the limit is not zero, then we have instability.

The study of the stability of the solution $\varphi_{p-k}^{(t)}$ can be reduced to that of the zero solution of another system analogous to (9), for example that relating to deviations $\varepsilon_{j-n}^{(t)}$.

$$\frac{d\varepsilon_{j-n}^{(t)}}{dt} = \Psi_{j-k}^{(t)}(\varepsilon_{j-1}^{(t)}, \varepsilon_{j-2}^{(t)}, \dots, \varepsilon_{j-n}^{(t)}, t) \quad (13)$$

(where $\Psi_{j-k}^{(t)}(0, 0, \dots, t) = 0$.)

The point $\varepsilon_{j-n}^{(t)} = 0$ is a resting point of equation (13). Applying stability theory, in the sense of Lyapunov, to the resting point leads to the following formulations.

It is said that the equilibrium point $\varepsilon_{j-n}^{(to)} = \varepsilon_{j-n}^{(t)}$ is stable in the Lyapunov sense if, $\forall \lambda > 0$,

$\exists \delta(\lambda) > 0 \wedge \forall \varepsilon_{j-n}^{(t)}$, solution of (13) whose initial values $\varepsilon_{j-n}^{(to)} = \varepsilon_{j-n}^{(t)}$ satisfy the conditions:

$$\forall \lambda > 0 \quad |\varepsilon_{j-n}^{(to)}| < \delta(\lambda) \quad (14)$$

We have inequality:

$$|\varepsilon_{j-n}^{(t)}| < \lambda \quad (15)$$

The equilibrium point $\varepsilon_{j-n}^{(t)} = 0$ is said to be unstable if, for any $\delta(\lambda) > 0$ no matter how small, the inequality $|\varepsilon_{j-n}^{(t)}| < \lambda$ is not satisfied for at least one solution $\varepsilon_{j-n}^{(t)}$. If, under condition (14), and in addition to inequality (15), the following condition is verified:

$$\lim_{t \rightarrow +\infty} |\varepsilon_{j-n}^{(t)}| = 0 \quad (16)$$

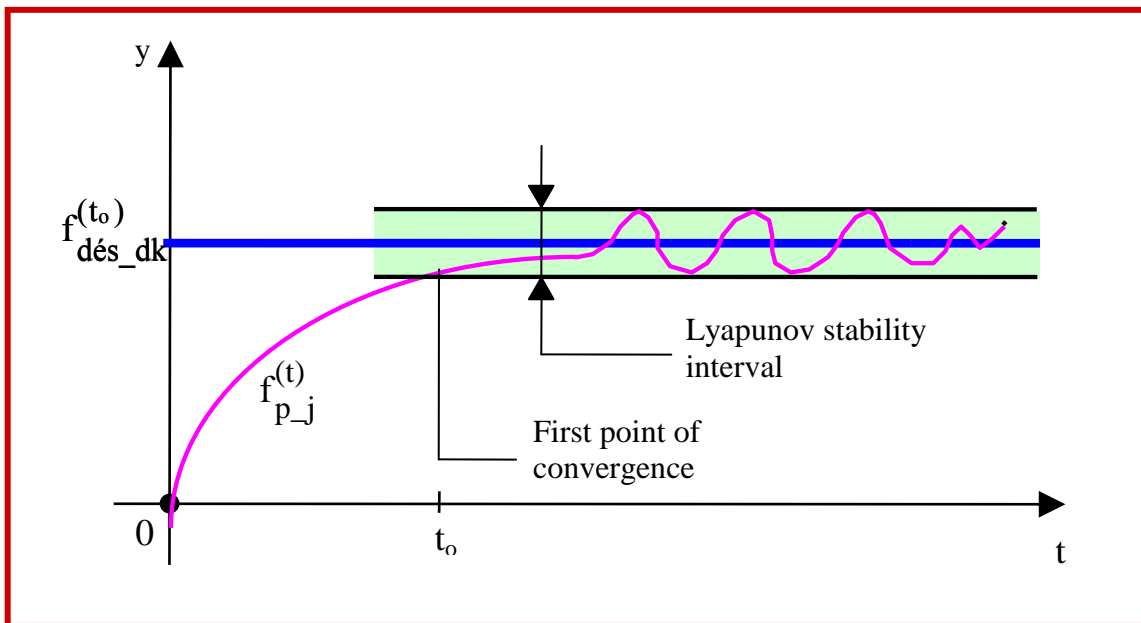
The solution $\varepsilon_{j-n}^{(t)}$ is said to be asymptotically stable.

These are the asymptotic stabilities (12) and (16) that must be obtained respectively for the outputs $A_{p-k}^{(t)}$ of neuron k and for the differences $\varepsilon_{j-n}^{(t)}$ between the output frequencies of

neurons d and j (or at the inputs of neuron k). We note that because the two systems are interdependent, satisfying one of the stabilities automatically satisfies the other.

The study of the asymptotic stability of $\varepsilon_{j-n}^{(t)}$ is equivalent to a study of the asymptotic stability of $f_{p-j}^{(t)}$ at the output of neuron j . The asymptote in this case is the line $y = f_{des-dk}^{(to)}$ toward which the successive values of $f_{p-j}^{(t)}$ must tend. Figure 6 below illustrates this stability. The stability interval is defined by the shaded area in the figure. The curve representing $f_{p-j}^{(t)}$ must evolve towards the asymptote $y = f_{des-dk}^{(to)}$, and stabilize in the vicinity of this asymptote. In other words, in the vicinity of the asymptote, if all other points relative to $f_{p-j}^{(t)}$ coming after the first point of convergence are included in the stability interval in the sense of Liapounov, we speak of convergence of $f_{p-j}^{(t)}$ towards $f_{des-dk}^{(to)}$. Otherwise, divergence occurs.

Figure 6: Illustration of $f_{p-j}^{(t)}$ convergence toward the asymptote $f_{des-dk}^{(to)}$.



Convergence occurs when the successive values of $f_{p-j}^{(t)}$ after the first point of convergence remain within the stability interval, in the sense of Liapounov, regardless of time t .

We must therefore establish conditions to obtain convergence of $f_{p-j}^{(t)}$ toward $f_{des-dk}^{(to)}$, followed by stabilization of $f_{p-j}^{(t)}$ at around $f_{des-dk}^{(to)}$; this amounts to ensuring that equation (16) is verified. Since the behavior of neuron j is not explicitly known in terms of its output potential values, it is not easy to establish these conditions analytically. Hence the necessity and importance of neuron k , which replaces the conditions to be established and must behave as a stabilizer (or regulator) in the Liapunov sense of the output value $f_{p-j}^{(t)}$ in the vicinity of

the asymptotic value $f_{des-dk}^{(to)}$. This justifies the use of the architecture in the form of a control system with a feedback loop, where the role of regulator of neuron k (see Figure 5).

In order for neuron k to perform its regulatory function, this second part of the algorithm that characterizes the behavior of neuron k is formulated as follows:

- 13) We define the input information for neuron k. As illustrated in the figure above, the presynaptic potentials at the input of neuron k are respectively the output potential $P_{p-j}^{(t)}$ of neuron j and the desired output potential $f_{des-dk}^{(to)}$ of neuron d. Neuron k integrates this information and innervates in the form of potential differences at the synaptic levels. Assuming that neuron k is doubly sensitive to variations in frequency and amplitude, we designate these respective sensitivities by $\mu_k^{(t)}$ and $\nu_k^{(t)}$.

- 14) At the synaptic level, stimulated by j, neuron k innervates in the form of a potential difference as follows:

$$dP_{s-jk}^{(t)} = \mu_k^{(t)} A_{ps-jk}^{(t)} df_{ps-jk}^{(t)} + \nu_k^{(t)} f_{ps-jk}^{(t)} dA_{ps-jk}^{(t)} \quad (17)$$

- 15) The resulting synaptic potential difference $dP_{r-k}^{(t)}$ at the input of neuron k is calculated (see Figure 5).

$$dP_{r-k}^{(t)} = \sum_1^n \left(\mu_k^{(t)} A_{ps-jk}^{(t)} df_{ps-jk}^{(t)} + \nu_k^{(t)} f_{ps-jk}^{(t)} dA_{ps-jk}^{(t)} \right) + \nu_k^{(t)} dA_{des-dk}^{(t)} f_{des-dk}^{(t)} \quad (18)$$

(where n is the number of synaptic contacts between the postsynaptic neuron k and the axonal terminals of presynaptic neurons j and d. It is assumed that the potential difference $dP_{des-dk}^{(to)}$ generated by d at k is constant. In other words, $dA_{des-dk}^{(to)}$ and $f_{des-dk}^{(to)}$ are known).

- 16) We calculate the difference in the intrinsic potential $dP_{p-k}^{(t)}$ of neuron k (see Figure 5).

$$dP_{p-k}^{(t)} = \Gamma(dP_{r-k}^{(t)}) = \left[2 / \left(1 + \exp(dP_{r-k}^{(t)}) \right) \right] - 1 \quad (19)$$

(where Γ is the behavior function of neuron k).

- 17) We assume that because the axon terminal of neuron k is in contact with that of neuron i, neuron k adjusts its output frequency to that of neuron i; this allows us to write the following equation:

$$f_{p-k}^{(t)} = f_{ps-ij}^{(t)} \quad (20)$$

(where $f_{ps-ij}^{(t)}$ is the output frequency of neuron i, and consequently the input frequency of neuron j).

So, the potential difference $dp_{p-k}^{(t)}$ becomes a function only of the amplitude variation $dA_{p-k}^{(t)}$ at the output of k (see Figure 5). It is this amplitude variation that will modify the amplitude at the output of neuron i , and consequently at the input of j .

- 18) We determine the variation in natural amplitude $dA_{p-k}^{(t)}$ of neuron k . Given that we know its output frequency from equation (20), the output amplitude is obtained by dividing the output potential by this frequency, i.e.:

$$dA_{p-k}^{(t)} = dP_{p-k}^{(t)} / f_{p-k}^{(t)} = dP_{p-k}^{(t)} / f_{ps-ij}^{(t)} \quad (21)$$

- 19) We calculate the modified input amplitude of neuron i at time $t + 1$. It results from adding the output amplitude of neuron i (or the input of neuron j) and the sum of the amplitude differences $dA_{p-k}^{(t)}$ of neuron k , which gives:

$$A_{ps-ij}^{(t+1)} = A_{ps-ij}^{to} + \sum_{t=0}^{t=N} dA_{p-k}^{(t)} \quad (22)$$

(where N is the number of iterations preceding the current iteration at time $t+1$).

- 20) The process is repeated from step 3 to step 19 as many times as necessary to obtain convergence of the output value $f_{p-j}^{(t)}$ of neuron j to the asymptotic value $f_{des-dk}^{(to)}$ of neuron d . To illustrate this convergence, simulations are performed and presented in the following section.

2-3. Validation of the model in terms of convergence and stabilization in the sense of Lyapunov

The aim is to show that the output value $f_{p-j}^{(t)}$ converges towards the desired value $f_{des-dk}^{(to)}$ and remains stable after the first convergence point, regardless of the number of subsequent iterations.

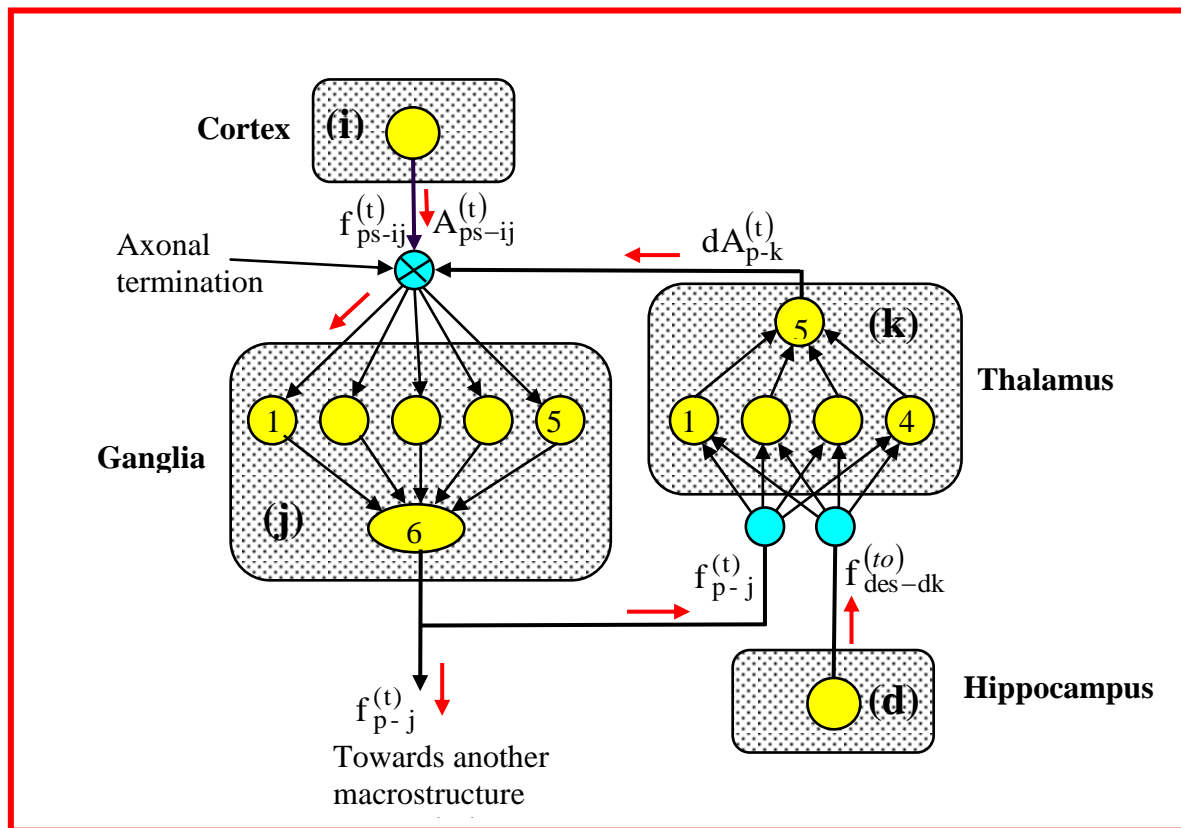
To illustrate this situation, we considered a simple architecture as shown in Figure 7 below, relating to the preparation of movement execution. In order to reduce the number of iterations and increase the performance of the model, several neurons were used at the macrostructure levels (j) and (k). We also assume that neurons i , j , k , and d belong to respective macrostructures such as:

- 1) the cerebral cortex (i) where movement is planned;
- 2) the basal ganglia (j) where it is programmed, and the program routed to the thalamus (k);
- 3) the hippocampus (d), which provides an old stored movement program to the thalamus (k);
- 4) and finally the thalamus (k), which compares the programs emanating from the basal ganglia (j) and the hippocampus (d), then provides the axonal termination of neuron i with the information needed to correct the discrepancy it has observed.

The process is repeated iteratively until the ganglia program (d) and the hippocampus program (d) are identical (zero deviation). From this point on, the program is sent to the cerebellum, the brain stem, and then to the spinal cord for execution by the muscles.

Regarding the architecture used, we note that the model shown in Figure 7 below incorporates the essential elements of Figures 2 and 4. An analogy can easily be drawn between the elements in Figure 5 and those in Figure 7, with the only difference being that in (i) and (j) there are more neurons, which does not change the functional principle of the model. It simply increases the performance of the system. From a macrostructural point of view, each neuron or group of neurons is assumed to belong to components of the system shown in Figure 7: the cortex (i), the ganglia (j), the hippocampus (d), and the thalamus (k).

Figure 7. Neural architecture used to validate the model.



2-3-1. Initial conditions of the model

Initial conditions were defined for the model parameters. They are shown in Tables 1 and 2 below. For the desired output frequency $f_{des-dk}^{(to)}$, the value chosen is 0.6.

Tableau 1 : Initial conditions
for ganglia (j).

Neurons	$\eta_j^{(to)}$	$\sigma_j^{(to)}$	$A_{s-ij}^{(0)}$
1	0.7	4	4
2	0.6	0.35	0.1
3	0.9	0.25	0.012
4	1.13	0.2	0.11
5	0.48	0.01	0.9
6	0,3	0,4	0,6

Tableau 2 : initial conditions for
the thalamus (k).

Neurons	$\mu_k^{(to)}$	$v_k^{(to)}$	$A_{s-kj}^{(0)}$
1	0.8	0	0.221
2	0.7	0	0.0034
3	0.8	0	0.001
4	0.02	0	0.1
5	0.7	0	0.3

2-3-2. Model behavior.

Figure 8 below clearly shows that the model works correctly in accordance with Lyapunov stability theory. The purple curve, representing the output frequency $f_{p-j}^{(t)}$ of the basal ganglia (j), converges and stabilizes at the blue asymptotic line representing the desired output frequency $f_{des-dk}^{(to)}$ of the hippocampus (k). In other words, the convergence time t_0 is such that: $\forall t \geq t_0$, conditions (12) and (16) of Lyapunov stability theory described in the previous section are verified. The green curve represents the evolution of the deviation (or error) $\varepsilon_j^{(t)}$ which tends towards zero as t tends towards infinity.

Figure 8. Illustration of model convergence and stabilization.

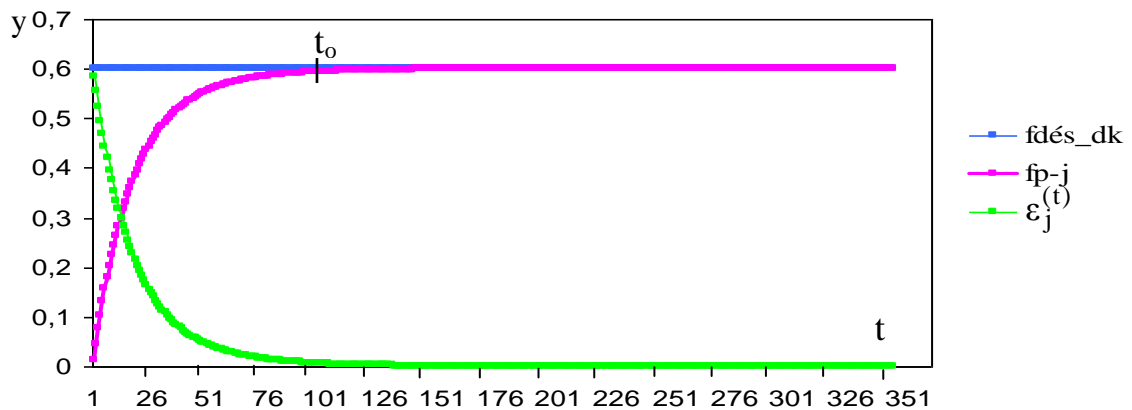
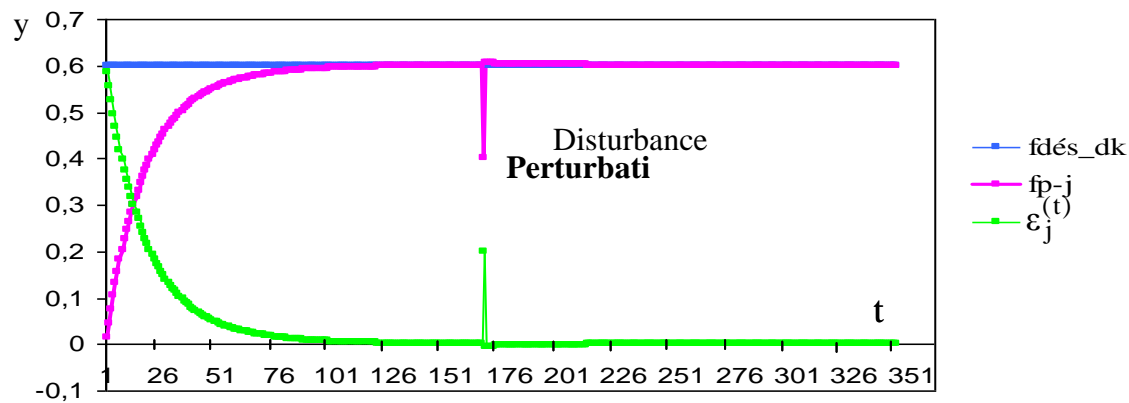


Figure 9 below shows a disturbance in the model at a given moment. This disturbance consists of abruptly changing the output frequency $f_{p-j}^{(t)}$ of (j). Once again, the model quickly corrects the error (deviation of $f_{p-j}^{(t)}$ far from $f_{des-dk}^{(to)}$) thus generated and stabilizes at the asymptotic line corresponding to $f_{des-dk}^{(to)}$. In view of these results, we can therefore confirm that the model presented in this article works perfectly in line with our expectations.

Figure 9. Illustration of model disturbance and restabilization.



Conclusion

As part of research into artificial intelligence, the aim of this work was to propose a mathematical model describing the functioning of feedback control systems or servomechanisms made up of components of the human brain.

With this model, which regulates the behavior of certain industrial processes or systems, and other neural network models capable of learning, memorizing, and retrieving data, we are still a long way from creating intelligent systems that resemble humans. Given the complexity of the neurobiological process underlying intelligence, other models will be developed in the future. These will focus on the simultaneous or sequential processing of information at several levels of the human brain, the way this information is routed between different macrostructures with specific functions, and the biological process of situation analysis, reasoning, and decision-making.

Bibliography

- [1] **Akinbusola Olushola^{1,*} and Victoria Alao²**, (2024). *Mathematical modeling of neural networks: Bridging the gap between mathematics and neurobiology*. World Journal of Advanced Engineering Technology and Sciences, 13(01), 516–526, <https://doi.org/10.30574/wjaets.2024.13.1.0448>.
- [2] **Changbao Wen; Jun Zha; Li Xu; Feng Ru; Si Quan**, (2024). *Research on Perceptron Neural Network Based on Memristor*. IEEE Transactions on Industrial Electronics (Volume: 71, Issue: 8, pp 9649 - 9657), DOI: 10.1109/TIE.2023.3319747.
- [3] **David Ottoson**, (1983). *Physiology of the nervous system*. Oxford University press, New York.
- [4] **Duane E. Haines**, (1995). *Neuroanatomy : An atlas of structures, sections, and systems*. Williams & Wilkins, 428 East Preston Street, Baltimore, Maryland 21202, USA, ISBN 0-683-03817-6.
- [5] **Edward R.Dougherty and Charles R. Giardina**, (1988). *Mathematical Methods for Artificial Intelligence and Autonomous systems*. Printice-Hall, Englewood Cliffs, New Jersey 07632, 1988, ISBN 0-13-560913-5.

- [6] **Eric R. Kandel, James H. Schwartz & Thomas M. Jessell**, (2000). *Principles of neural science*. Elsevier Science Publishing Co., Inc. 655 Avenue of the Americas, New York, NY 10010.
- [7] **Gordon M. Shepherd, Ed.** (1990). *The synaptic of the brain*. 3rd Edition, Oxford University Press.
- [8] **Ivan A. Bachelder and Allen M.; Waxman**, (1994). *Mobile robot mapping and localization : A view based neurocomputational architecture that emulates hippocampal place learning*. Neural Networks, vol. 7. No. 6/7. pp. 1083-1099.
- [9] **Jaswinder Singh & Rajdeep Banerjee**, (2019, March 27-29). *A Study on Single and Multi-layer Perceptron Neural Network*. The 3rd International Conference on Computing Methodologies and Communication (ICCMC), Erode, India | Conference Paper | Publisher: IEEE, DOI: 10.1109/ICCMC.2019.8819775.
- [10] **J. J. DI STEFANO, A.R. STUBBERUD, I. J. WILLIAMS**, (1974). *Systèmes asservis, cours et problèmes*. McGraw-Hill. 28, rue Beaunier, 75014 Paris, ISBN 2-7042-0017-3.
- [11] **J. J. Yin; Wallace K. S. Tang; K. F. Man**, (2010). *A Comparison of Optimization Algorithms for Biological Neural Network Identification*. IEEE Transactions on Industrial Electronics (Volume: 57, Issue: 3, pp 1127 - 1131), DOI: 10.1109/TIE.2009.2027254.
- [12] **Minoru Tsukeshi Aihara, Hides-Aki and Hiroshi Kato**, (1996). *Hippocampal LTP depends on spatial and temporal correlation of inputs*. Tamagawa University and Yamagata University, Japan ; Neural Networks, Vol. 9, No 8, pp. 1357-1365.
- [13] **Richard Drebin**. *On the correspondence between network models and the nervous system*. Nature 326, pp. 689-691.
- [14] **Robert RIGAL**, (1987). *Motricité humaine*. Presses, de l'Université du Québec, C.P. 250, Sillery (Québec), G1T 2R1 Canada, ISBN 2-7605-0379-8.
- [15] **Roheen Qamar^{1*} & Baqar Ali Zardari²**, (2023). *Artificial Neural Networks: An Overview*. Mesopotamian Journal of Computer Science, pp 130-139, DOI: 10.58496/MJCSC/2023/015.
- [16] **Roza Dastres, Mohsen Soorin**, (2021). *Artificial Neural Network Systems*. International Journal of Imaging and Robotics (IJIR), 21 (2), pp.13-25. fihal-03349542.
- [17] **Samuel Schmidgall, Rojin Ziaei, Jascha Achterberg, Louis Kirsch & S. Pardis Hajiseyedrazi**, (2024). *Brain-inspired learning in artificial neural networks: A review*. APL Mach. Learn. 2, 021501 (2024), <https://doi.org/10.1063/5.0186054>.
- [18] **Sibiri TRAORE and Michel GUILLOT**, (2007). *A learning algorithm based on the electrophysiology of human brain neurons*. Journal Africain de Communication Scientifique et Technologique, No 2, pp 41-55.

- [19] **Simon HAYKIN**, (1994). *Neural networks. A comprehensive foundation*. Macmillan College Publishing Company, New York, ISBN 0-02-352761-7.
- [20] **Steven J. Olson, Stefen Grossberg**, (1998). *A neural network model for the development of simple and complex cell receptive fields within cortical maps of orientation and ocular dominance*. Neural networks, vol. 11. No.2 pp. 189-208.